

# Statistical Evaluation of Nonlinear Distortion using the Multi-Canonical Monte Carlo Method and the Split Step Fourier Method

Ioannis Neokosmidis, Nikos Gkekas, Thomas Kamalakis, and Thomas Sphicopoulos

**Abstract**—In high powered dense wavelength division multiplexed (WDM) systems with low chromatic dispersion, four-wave mixing (FWM) can prove to be a major source of noise. The MultiCanonical Monte Carlo Method (MCMC) and the Split Step Fourier Method (SSFM) are combined to accurately evaluate the probability density function of the decision variable of a receiver, limited by FWM. The combination of the two methods leads to more accurate results, and offers the possibility of adding other optical noises such as the Amplified Spontaneous Emission (ASE) noise.

**Keywords**—Monte Carlo, Nonlinear optics, optical crosstalk, Wavelength-division Multiplexing (WDM).

## I. INTRODUCTION

THE growth of the Internet in the last years in terms of traffic volume, number of users and commercial applications is unrivalled in history. IP traffic follows an exponential growth and almost doubles every six months. Both Internet and telecommunications service providers realized the obvious need for a scalable networking technology to meet this ever-growing demand. Optical networks [1] have been adopted as an efficient means to accommodate this traffic increase, especially in the backbone and metro part of the network. State-of-the-art, Wavelength Division Multiplexing (WDM) systems, are designed to have a large number of closely spaced channels operating at 10 to 40Gb/s rates each. In such systems the linear and the nonlinear effects of the optical fibre can cause considerable performance degradation.

Four-Wave Mixing (FWM) is one of the most detrimental nonlinear effect in the case of non-zero dispersion fibers (NZDF) and narrow channel spacing ( $\Delta f_{ch} \leq 100\text{GHz}$ ) [2]. The statistical analysis of the decision variable at the receiver of a WDM system is of great importance for the network design and modeling. Through such an analysis the performance of the system can be evaluated.

In the literature, one can find several methods for the evaluation of the performance of a WDM system, limited by nonlinear effects and especially the FWM noise. Among these methods, the most popular are the MultiCanonical Monte simulations [3]-[5] and the Split Step Fourier Method (SSFM) [6]. The SSFM is a numerical method for the solution of the

nonlinear propagation equation governing the pulse evolution inside an optical fiber. According to this method, the fiber is segmented into small pieces of length  $h$ . In each piece, the linear and nonlinear effects are applied separately. The field at the end of each segment represents the input of the next segment. This technique is accurate since it can take into account all the propagation effects as well as the noise-noise interaction in the fiber without making any assumptions. However, the disadvantage of this method is that the obtained results can only give a first insight of the performance of the system. This is especially true when the distribution of the noise sources is not Gaussian. In this case the  $Q$ -factor evaluated from the eye diagrams obtained by the SSF can not be used for the estimation of the BER through the erfc function. The SSFM can ideally be used in order to estimate the PDF of the decision variable at the receiver. Due to the increased computational time, this method can not yield information about the tails of the PDF since the noise realizations in the simulation are picked in an unbiased manner.

On the other hand, the Probability Density Function (PDF) of the FWM noise or the decision variable can be easily calculated using the MCMC method. Using the MCMC simulations, one can quickly reveal the tails of the corresponding PDF. The advantage of this method is that it automatically determines the bias with an iterative procedure. This requires the knowledge of the decision variable in closed form. Sometimes, this requirement comes at the expense of making assumptions. Furthermore, the inclusion of other noises at this model is not always easy since this imposes the transformation of the equations describing the decision variable.

In this work the MMC method and the SSF method are combined to accurately evaluate the performance of a WDM system, limited by FWM noise. The rest of the paper is organized as follows: In section II.A, some basic considerations are given concerning the origin of the FWM phenomenon which will be used in section II.B to derive an expression for the photocurrent at the receiver. In section III the system under investigation is illustrated. The transmission model used to study the system under consideration is described in section IV. The MCMC method is presented in section V. The obtained results are shown and discussed in

section VI. The work is concluded in section VII.

## II. THEORETICAL BACKGROUND

### A. Four-Wave Mixing

Four-Wave Mixing (FWM) is included in the category of the nonlinear effects known as Kerr effects. These nonlinear effects originate from nonlinear refraction, a phenomenon that refers to the intensity dependence of the refractive index. In detail, FWM is due to the existence of third-order nonlinear polarization that is to the contribution of the third order nonlinear susceptibility  $\chi^{(3)}$ .

Considering three optical waves oscillating at frequencies  $f_i$ ,  $f_j$  and  $f_k$ . According to the FWM process, new optical waves can be generated from the nonlinear interaction of the three optical waves. The new optical waves (FWM products) are positioned at frequencies  $f_{ijk} = f_i + f_j - f_k$ . In a WDM system with equal channel spacing, the central frequency of the products will coincide with some of the central frequencies of the channels resulting to interchannel interference.

The output power  $P_{pqr}$  of the FWM product is given by [7]:

$$P_{pqr} = \frac{\gamma^2}{9} d_{pqr}^2 P_p P_q P_r e^{-aL} L_{eff}^2 \eta \quad (1)$$

where  $P_i$  ( $i = p, q, r$ ) represents the input peak power at the frequencies  $f_i = \omega_i/2\pi$  in the mark state. Assuming a perfect extinction ratio, the average input power is  $P_{av} = P_i/2$ . It should be noted that equation (1) is an approximation that holds since the power of the FWM components is very small compared with the signal power at each channel [8]. In a WDM system it can be assumed that all the peak powers at the mark state are equal ( $P_i = P_{in}$  for  $i=1,2,\dots,N$ ). In (1)  $\gamma$  is the nonlinear coefficient of the fiber [7],  $a$  is the fiber loss coefficient,  $L$  is the total fiber length,  $L_{eff} = (1 - e^{-aL})/a$  is the effective length of the fiber,  $d_{pqr}$  is the degeneracy factor ( $d_{pqr}=3$  when  $p=q$ ,  $d_{pqr}=6$  when  $p \neq q$ ) and  $\eta$  is the mixing efficiency given by:

$$\eta = \frac{a^2}{a^2 + (\Delta\beta)^2} \left\{ 1 + \frac{4e^{-aL} \sin^2(\Delta\beta L/2)}{[1 - e^{-aL}]^2} \right\} \quad (2a)$$

In (2a),  $\Delta\beta$  represents the phase mismatch and may be expressed in terms of the channel frequencies  $f_i$ :

$$\begin{aligned} \Delta\beta &= \frac{2\pi\lambda^2}{c} (f_p - f_r)(f_q - f_r) \cdot \\ &\cdot \left\{ D(\lambda_o) + \frac{dD(\lambda_o)}{d\lambda} \left( \frac{\lambda^2}{2c} \right) ((f_p - f_o) + (f_q - f_o)) \right\} \\ &= \frac{2\pi\lambda^2}{c} \Delta f^2 (p-r)(q-r) \cdot \\ &\cdot \left\{ D(\lambda_o) + \frac{dD(\lambda_o)}{d\lambda} \left( \frac{\lambda^2}{2c} \right) \Delta f ((p-o) + (q-o)) \right\} \end{aligned} \quad (2b)$$

or approximately,

$$\Delta\beta \approx \frac{2\pi\lambda^2 D}{c} \Delta f^2 (p-r)(q-r) \quad (2c)$$

In (2b),  $D$  is the fiber chromatic dispersion coefficient,  $\lambda$  is the wavelength of the signal and  $c$  is the speed of light in vacuum. Equation (2c) is derived using the fact that for typical values of  $D$ ,  $dD/d\lambda$  and  $\Delta f$ , the second term in the brackets is much smaller than the first one [9].

The amplitude of the optical fields  $E^{(m)}$  and  $E^{(s)}$ , in the mark and the space state respectively, at a given channel  $n$  is written as [10]:

$$E^{(m)} = \sqrt{P_n e^{-aL}} \exp[j\theta_n] + \sqrt{P_{F(IM)}^{(m)}} \exp[j\theta_{F(IM)}^{(m)}] \quad (mark) \quad (3a)$$

$$E^{(s)} = \sqrt{P_{F(IM)}^{(s)}} \exp[j\theta_{F(IM)}^{(s)}] \quad (space) \quad (3b)$$

where  $P_n$  and  $\theta_n$  are the input peak power and the phase in the mark state, respectively, of the given channel  $n$  and

$$\begin{aligned} \sqrt{P_{F(IM)}^{(m)}} \exp[j\theta_{F(IM)}^{(m)}] &= \sum_{p \neq q \neq r \neq n} B_p B_q B_r \sqrt{P_{pqr}} e^{j\theta_{pqr}} + \\ &+ \sum_{p \neq q \neq r = n} B_p B_q \sqrt{P_{pqn}} e^{j\theta_{pqn}} + \sum_{p = q \neq r} B_p B_r \sqrt{P_{ppr}} e^{j\theta_{ppr}} \\ \sqrt{P_{F(IM)}^{(s)}} \exp[j\theta_{F(IM)}^{(s)}] &= \end{aligned} \quad (4a)$$

$$= \sum_{p \neq q \neq r \neq n} B_p B_q B_r \sqrt{P_{pqr}} e^{j\theta_{pqr}} + \sum_{p = q \neq r} B_p B_r \sqrt{P_{ppr}} e^{j\theta_{ppr}} \quad (4b)$$

while  $P_{pqr}$  and  $\theta_{pqr} = \theta_p + \theta_q - \theta_r$  are the peak power and the phase of the FWM noise generated from a channel combination ( $p, q, r$ ). The above sums run for all integers  $p, q, r$  that satisfy the condition  $p+q-r=n$  (which is imposed by an energy conservation requirement) and the restrictions shown in (4a) and (4b). These restrictions can be summarized as  $r \neq p, q$  which guarantees that the corresponding term is not due to SPM or XPM. Furthermore,  $B_i = 0$  or  $B_i = 1$  is the bit value of channel  $i$ . These expressions for the electric field will be used in the next section in order to derive an expression for the photocurrent at the receiving photodiode.

### B. Calculation of the Photocurrent

At the receiver, the photocurrent is proportional to the optical power and hence to  $|E|^2$  where  $E = E^{(m)}$  or  $E = E^{(s)}$  [11]. In practical applications, it can be assumed that  $\Delta\beta \gg a$ , which generally holds for  $D \geq 2\text{ps/nm/Km}$  and channel spacing  $\Delta f \geq 10\text{GHz}$ . For large  $L$  one can also use the fact that  $\exp(-aL) \ll 1$ . Assuming a single fiber span without optical amplification, all other noises at the receiver except FWM can be ignored. This is especially true for high input powers and in this case the photocurrent at the detector is written as:

$$S^{(m)} = k |E^{(m)}|^2 \approx k P_n e^{-aL} + 2k \delta \sqrt{P_n e^{-aL}} I_m \quad (5a)$$

$$S^{(s)} = k |E^{(s)}|^2 \approx k \delta^2 I_s \quad (5b)$$

where  $k$  is the receiver responsivity and

$$\delta = \frac{\gamma c}{2\pi\lambda^2 D\Delta f^2} P_{in}^{\frac{3}{2}} e^{-aL/2} \quad (6a)$$

$$I_m = \frac{1}{3} \sum_{pqr} B_p B_q B_r \frac{d_{pqr}}{|p-n||q-n|} \cos(\theta_{pqr} - \theta_n) \quad (6b)$$

$$I_s = \left( \frac{1}{3} \sum_{\substack{pqr \\ r \neq n}} B_p B_q B_r \frac{d_{pqr}}{|p-n||q-n|} \cos \theta_{pqr} \right)^2 + \left( \frac{1}{3} \sum_{\substack{pqr \\ r \neq n}} B_p B_q B_r \frac{d_{pqr}}{|p-n||q-n|} \sin \theta_{pqr} \right)^2 \quad (6c)$$

Equations (5a) and (5b) provide an expression for the photocurrent in the mark and space state in terms of two new variables  $I_m$  and  $I_s$  given by (6b) and (6c) respectively. It is interesting to note that for a given number of channels, these new variables depend only on the bits and the phases of the optical signals.

### III. SYSTEM DESCRIPTION

A WDM multi-span system consisting of  $N \times 10$  Gb/s channels with channel spacing  $\Delta f_{ch}$  is assumed (figure 1). The transmission line is composed of four 80-km spans of G.655 fiber, each followed by an in-line EDFA optical amplifier (having a noise figure of 4 dB) containing dispersion compensating fiber (DCF) module (0.8km each). The gain of the amplifiers is equal to the fiber losses in each span. The G.655 fiber is assumed to have  $D=2$  ps/nm/km, optical loss coefficient  $a_{dB}=0.2$  dB/km and a non-linear coefficient  $\gamma=2$  (W×km)<sup>-1</sup>. The DCF has  $D=-200$  ps/nm/km,  $a_{dB}=0.5$  dB/km and  $\gamma=4.5$  (W×km)<sup>-1</sup>. At the receiver the signals are demultiplexed using a DEMUX with a Gaussian characteristic. Each signal is then detected using a direct detection receiver.

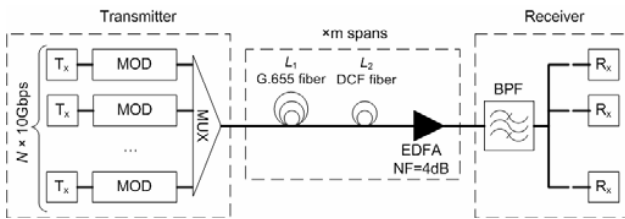


Fig. 1 System under investigation

The input optical power waveform representing a single “1”-bit,  $p_1(t)$  is specified within the time interval  $[0, (1+b)T_p]$  as [12]:

$$p_1(t) = \begin{cases} \frac{P_{in}}{2} \left[ 1 - \sin \left( \frac{\pi}{bT_p} \left( t - (1+b)\frac{T_p}{2} - \frac{T_p}{2} \right) \right) \right], & t \in [0, bT_p] \text{ and } [T_p, (1+b)T_p] \\ P_{in}, & t \in [bT_p, T_p] \end{cases} \quad (7)$$

where  $P_{in}$  denotes the peak input power,  $T_p$  represents the bit duration and  $b$  specifies the pulse shape. Note that  $p_1(t)$  rises from 0 to  $P_{in}$  within  $[0, bT_p]$ , remains constant and equal to  $P_{in}$  within  $[bT_p, T_p]$  and then falls from  $P_{in}$  to zero within  $[T_p, (1+b)T_p]$ . Varying  $b$  from 1 to 0, the pulse shape changes from  $\cos^2(t)$ -like to rectangular. Throughout this work NRZ pulses are used with a value of  $b=0.4$ . Finally, the bit duration  $T_p$  was taken to be 100ps corresponding to an ASK bit rate  $R_{ASK}=10$  Gbps. The central channel of the WDM system is assumed to be located around  $\lambda_0=1.55\mu\text{m}$ .

### IV. THE TRANSMISSION MODEL

In order to test the performance of the system, the fiber's propagation equation can be numerically solved using the Split Step Fourier Method (SSFM) [6, pp. 51-53]. The basic propagation equation is written as:

$$\frac{\partial A}{\partial z} = -\frac{j}{2} \beta_2 \frac{\partial^2 A}{\partial t^2} - \frac{\alpha}{2} A + j\gamma |A|^2 A \quad (8)$$

where  $A=A(t,z)$  is the slowly varying complex envelope of the optical field at time  $t$  and position  $z$  along the fiber,  $\beta_2$  is the Group Velocity Dispersion (GVD) parameter,  $\alpha=a_{dB}/4.343$  is the fiber loss coefficient and  $\gamma$  is the nonlinear coefficient of the fiber.

In an  $N$ -channel WDM system, the input signal ( $z=0$ ) can be written as:

$$A(t,0) = \sum_{i=1}^N A_i(t,0) e^{j2\pi f_i t} \quad (9)$$

where  $A_i(t,0)$  and  $f_i$  are the slowly varying envelope and the central frequency of the  $i$ -th channel respectively. Equation (8) under the initial condition (9), can be used to describe the signal propagation taking into account the optical losses, chromatic dispersion and the three Kerr-induced nonlinear phenomena, namely the SPM, XPM and FWM effects.

In order to investigate the performance of a WDM system, the  $Q$ -factor can be calculated from the eye diagrams at the receiver. The  $Q$ -factor is a commonly used parameter in telecommunications and it is expressed as:

$$Q = \frac{\langle P_1 \rangle - \langle P_0 \rangle}{\sigma_1 + \sigma_0} \quad (10)$$

where  $\langle P_1 \rangle$  and  $\langle P_0 \rangle$  are the average optical power of bits “1” and “0” respectively and  $\sigma_1$  and  $\sigma_0$  are the corresponding standard deviations of the noise. In the case where the PDFs of the decision variable at the receiver, both at the mark and the space state, follow the Gaussian distribution the value of the  $Q$ -factor can be used to evaluate the BER of the system:

$$BER = \frac{1}{2} \operatorname{erfc} \left( \frac{Q}{\sqrt{2}} \right) \quad (11)$$

All channels are assumed aligned in time at the input (synchronous WDM system) and equally spaced. Under these conditions the strength of FWM effect is maximized, especially in the case of RZ pulses [13]-[14]. When NRZ pulses are used however, the synchronization of the bits does not seem to affect the system performance [14].

## V. MULTICANONICAL MONTE CARLO METHOD

The MCMC method can be used to numerically calculate the probability density function (PDF) of a random variable. MCMC is a fast and accurate statistical method useful for the evaluation of even very low error probabilities. MCMC simulations are Monte Carlo simulations with a-priori unknown weights. According to this method the interval  $K$ , in which the variable  $S$  of interest takes its values, is divided into small subintervals  $S_0, \dots, S_P$  and a histogram  $H_k$  is used to measure the occurrences of  $S$  that fall inside each subinterval  $S_k$ . For simplicity, the length of  $S_k$  can be taken constant and equal to  $\Delta s$ . On each iteration  $i$  of the MCMC method, the estimated PDF of  $S$  is stored in the variables  $P_k^i$ , and, as the number of iterations increases,  $P_k^i \rightarrow P_k$  where  $P_k = P(S \in S_k)$ .

In each iteration  $i$ , the occurrences of  $S$  inside each interval  $S_k$  are recorded in the histograms  $H_k^i$ . At the end of the iteration, the values of the  $P_k^i$  are updated according to the values of the  $H_k^i$  using the recurrence relations [15]:

$$P_{k+1}^{i+1} = \frac{P_{k+1}^i P_k^{i+1}}{P_k^i} \left( \frac{H_{k+1}^i}{H_k^i} \right)^{g_k^i} \quad (12)$$

where the exponents  $g_k^i$  are given by

$$g_k^i = \frac{f_k^i}{\sum_{h=1}^i f_k^h}, \quad f_k^h = \frac{H_k^h H_{k+1}^h}{H_k^h + H_{k+1}^h} \quad (13)$$

It should be noted that  $g_k^i=0$ , if  $f_k^i=0$ . Also,  $f_k^h=0$ , if  $H_k^h+H_{k+1}^h=0$ . The  $P_k^i$  are normalized so that their sum with respect to  $k$  is equal to unity. For  $i=1$  the values of  $P_k^i = P_k^1$  are all set equal to  $1/P$ , which means that the first iteration corresponds to standard Monte Carlo sampling. As  $i$  increases, the information gained for the PDF of  $S$  through the  $P_k^i$ , is used to bias the samples and increase the occurrence of the values of  $S$  at the tails of its PDF. After the final iteration  $i=Q$ , the values of  $P_k^Q$  provide an estimate for  $f_S(s)$  and are normalized so that  $\Delta s \sum_{k \geq 1} P_k^Q = 1$ .

The random samples of  $S$  are generated by the Metropolis algorithm [5]. The BER is calculated by performing numerical integration of the corresponding PDFs using equation (10).

$$P_e(Q_{th}) = \frac{1}{2} \int_{-\infty}^{Q_{th}} f_S^{(s)}(x) dx + \frac{1}{2} \int_{Q_{th}}^{\infty} f_S^{(m)}(x) dx \quad (14)$$

where  $Q_{th}$  is the threshold at the receiver. The value of  $Q_{th}$  is chosen so that the BER is minimized.

## VI. RESULTS AND DISCUSSION

### A. Application of the MCMC Method

In this section, the MCMC method will be applied for the estimation of the PDFs of  $I=I_s$  and  $I=I_m$  of a WDM system. Once the PDF of  $I_m$  and  $I_s$  is determined, the PDF of  $S^{(m)}$  and  $S^{(s)}$  can also be determined, using the theorem of transformation of random variables [16]. The optical phases of all channels are assumed to be uniformly distributed within  $[0, 2\pi]$ , due to phase noise [11], and the data bits are assumed to be in the mark and space state with equal probability,  $P(B_i=0)=P(B_i=1)=1/2$ . The number of iterations used was  $Q=20$  and each iteration involved the generation of 50000 samples.

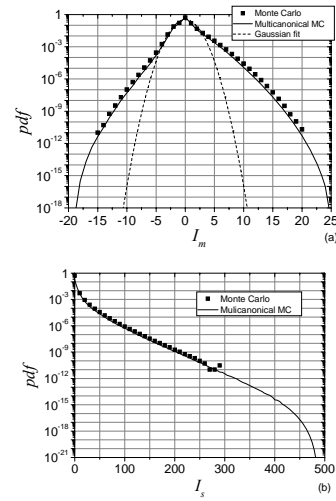


Fig. 2 The PDFs of a)  $I_m$  and b)  $I_s$  for  $N=16$  calculated using the MCMC (solid lines) and conventional MC (dots) methods. Also shown with dotted lines in (a) is a Gaussian distribution with the same standard deviation as  $I_m$

The results obtained by the MCMC method for the central channel ( $n=8$ ), of a sixteen channel WDM system, are plotted with solid lines in Fig. 2 for the case where a) the signal bit  $B_n$  is "1" ( $I=I_m$ ) and b) the signal bit  $B_n$  is "0" ( $I=I_s$ ). Also shown with dots are the PDFs obtained by the conventional Monte-Carlo method. For each PDF, it took the MCMC algorithm about  $10^3$  times less time than the conventional MC method to complete its calculations for values of the PDF up to  $10^{-10}$ . It is therefore deduced that the MCMC method can decrease the computation time by many orders of magnitude. It is also interesting to note that the MCMC method required only  $10^6$  samples in order to evaluate the PDF values as low as  $10^{-18}$ . Conventional MC would require at least  $10^{19}$  samples in order to evaluate these values of the PDF making the computation extremely time consuming. Hence, the MCMC method can be used to estimate even very low error probabilities (i.e.  $10^{-14}$ ), which cannot be computed using conventional MC sampling. Finally the BER can be estimated using the PDFs  $S_m$  and  $S_s$ .

and applying numerical integration. For example, in the case of a single span system with fiber length  $L=80\text{km}$ , chromatic dispersion  $D=2\text{ps/nm/km}$ , channel spacing  $\Delta f=50\text{GHz}$ , input peak power  $P_m=10\text{dBm}$ , fiber losses  $\alpha=0.2\text{dB/km}$  and  $N=16$  channels the BER equals to  $10^{-7}$ .

Another approach is to approximate the PDF with a Gaussian distribution. This is illustrated in figure 2(a) where a Gaussian PDF with the same standard deviation is plotted with dashed lines. It is evident that the Gaussian PDF fails to approximate the PDF of  $I_m$  especially for values below  $10^{-4}$  and hence the Gaussian distribution cannot accurately describe the PDF. This is because the FWM noise is a sum of a large number of components (eqs. 5-6), dependent on each other. Hence, the central limit theorem, on which the Gaussian approximation is based, is not valid in this case.

The MCMC can also be used in order to estimate the PDF of the FWM in both states in a multi-span WDM system. A more general approach is to carry out the MCMC simulations using the multi-span FWM efficiency formula given in [17]. According to this method, the efficiency of the FWM process must be multiplied by  $\sin(M\Delta\beta L/2)/\sin(\Delta\beta L/2)$  where  $M$  is the total span number,  $\Delta\beta_{\text{pqr}}$  is the phase mismatch factor of each product and  $L$  is the length of each span. However, this formula imposes that all the fiber spans must have the same length leading to limited accuracy.

#### B. Application of the Split-Step Fourier Method

To estimate the performance of the system, the input channels will be assumed modulated by a  $2^8-1$  pseudorandom bit streams and a series of simulations were carried out using the SSFM method. The bandwidth  $\Delta B$  of the optical demultiplexer was optimized at the receiver using numerical simulations.

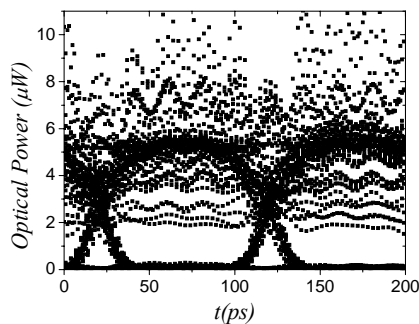


Fig. 3 Eye diagrams for the central channel of a single span eight-channel WDM system. The transmission rate is 10Gb/s, the channel spacing is 50GHz and the input power is 10dBm

In Fig. 3, the eye diagram for the 5<sup>th</sup> channel (central channel) of a single span eight-channel WDM system is shown. A 10Gb/s WDM system is assumed, with channel spacing equal to 50GHz, fiber length  $L=160\text{km}$  and input peak power 10dBm. This figure provides a first indication of the performance of the system. As depicted in Fig. 3, the eye-diagram is closed due to the effect of the FWM induced distortion. The  $Q$ -factor in this case is 3.4 resulting in a high

error probability. If the FWM is assumed to follow Gaussian distribution, this  $Q$ -factor corresponds to an error probability of  $\text{erfc}(Q/\sqrt{2})/2 \approx 3 \times 10^{-4}$ .

Using the transmission model and the SSF method, one can also include other noises such as the ASE noise due to optical amplifiers. The parameters of the transmission line are as follows:  $m=4$  spans,  $L_1=80\text{km}$ ,  $L_2=0.8\text{km}$ , noise figure (EDFA) 4 dB. The gain of the amplifiers is equal to the fiber losses in each span.

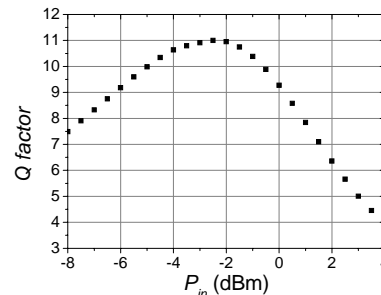


Fig. 4  $Q$  factor as a function of input peak power

Fig. 4 illustrates the  $Q$  factors of the worst channel which turns out to be one of the center channels (channels 4 and 5), which suffer the most due to FWM. In the low power region, the ASE noise limits the system performance. As the power rises the signal to noise is increased. At some point however, the nonlinear effects become important and begin to deteriorate the  $Q$  factor. Therefore, there is an optimum input power corresponding to the maximum  $Q$  factor. The maximum  $Q$  factor obtained by is 11. Assuming that the PDF of the FWM noise follows the Gaussian distribution, the optimum  $Q$  factor corresponds to  $\text{BER}=1.9 \times 10^{-28}$ .

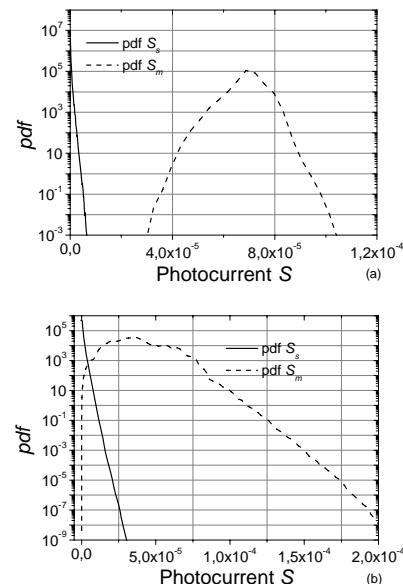


Fig. 5 Probability density function of the photocurrent at the receiver in the case of a) single span system with  $P_m=5\text{dBm}$  and b) multispan system with  $P_m=2\text{dBm}$

### C. Combining the MCMC and the SSF Methods

In this section the MCMC and the SSF method are used in order to evaluate the PDF of the photocurrent at the receiver as well as the BER of the system. In each iteration, a series of SSF simulations are performed. The SSFM is used in order to propagate the optical pulses. The received pulses are used to estimate the photocurrent. The photocurrent is calculated by averaging the field amplitude over a small area around the center of the middle pulse. At the end of each SSF simulation, the occurrences of the photocurrent values are recorded in a histogram which leads to the calculation of the PDF of the photocurrent. Two cases are investigated. The first one is a single span system with dispersion compensation and without amplification while the second one is a four span system with amplification. The parameters of the systems are as in section III.B.

To estimate the performance of the system, the input channels will be assumed modulated by a pseudorandom bit stream of 16bits. The number of the transmitted pulses is sufficient, exhausting all the possible bit patterns around the signal bit. This is because there is a small shift of the channels due to the dispersion.

Fig. 5 illustrates the PDFs of the photocurrent at the receiver based on many MCMC noise realizations a) single span system and b) multispan system. In both cases, the PDFs have the same shape as in the case of Fig. 3. This fact indicates that the FWM is the dominant noise source even if the ASE noise and the other nonlinearities are present. It is also interesting that the inclusion of more spans as well as the optical amplification enforces the effect of the FWM noise. This was expected since the FWM products, generated in a span, are amplified by the EDFA. Furthermore, these products constitute signals that participate in the FWM process of the next span. Finally, it can also be mentioned that the PDFs are far way from the Gaussian distribution.

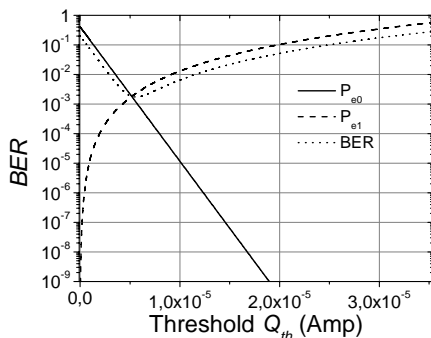


Fig. 6 BER as a function of the photocurrent. The functions  $P_{e0}$  and  $P_{e1}$  are also shown. The BER equals half the sum of the two

The knowledge of the PDFs of the mark and space state allows us to calculate the bit error probabilities (eq. 14). The two integrals correspond to the probability  $P_{e0}$  ( $P_{e1}$ ) of receiving a mark (space), when a space (mark) was transmitted. The BER becomes minimal at the optimal decision level  $Q_{th,opt}$ . Figure 6 shows  $P_{e0}$  and  $P_{e1}$  as well as the

BER as a function of the threshold. The optimum decision level lies at  $Q_{th,opt}=5.59 \times 10^{-6}$  Amp near the intersection of the two curves ( $P_{e0}$  and  $P_{e1}$ ) and yields a BER of  $1.736 \times 10^{-3}$ .

### VII. CONCLUSION

The Split-Step Fourier method and the MultiCanonical Monte Carlo method are combined to evaluate the performance of a WDM system. MCMC is a fast statistical method useful for the evaluation of even very low error probabilities. On the other hand, the solution of the nonlinear propagation equation using the SSF method leads to very accurate results since it takes into account all the propagation effects as well as the noise-noise interaction in the fiber without making any assumption. Hence, the resultant method is able to accurately compute the complete PDF of the decision variable at the receiver. Finally, the BER of the system is estimated using numerical integration of the obtained PDFs.

### REFERENCES

- [1] R. Ramaswami and K. Sivarajan, *Optical Networks: A Practical Perspective*. San Diego: Academic Press, 2002.
- [2] I. Neokosmidis *et al.*, "New Techniques for the Suppression of the Four-Wave Mixing-Induced Distortion in Nonzero Dispersion Fiber WDM Systems," *J. Lightwave Technol.*, vol. 23, No. 3, pp. 1137-1144, 2005.
- [3] D. Yevick, "Multicanonical Communication System Modeling – Application to PMD statistics," *IEEE Photon. Tech. Letters*, Vol. 14, pp. 1512-1514 (2002).
- [4] R. Hozhonner *et al.*, "Use of multicanonical Monte Carlo simulations to obtain accurate bit error rates in optical communication systems," *Optics Lett.*, Vol. 28, pp. 1894-1896 (2003).
- [5] David P. Landau and K. Binder, *A Guide To Monte Carlo Simulations in Statistical Physics*, Cambridge: Cambridge University Press, 2002.
- [6] G. P. Agrawal, *Nonlinear Fiber Optics*, 2<sup>nd</sup> ed. N.Y.: Academic, 1995
- [7] S. Song, C. T. Allen, K. R. Demarest and R. Hui, "Intensity-Dependent Phase-Matching Effects on Four-Wave Mixing in Optical Fibers," *J. Lightwave Technol.*, Vol. 17, pp. 2285-2290 (1999).
- [8] K. O. Hill, D. C. Johnson, B. S. Kawasaki and R. I. MacDonald, "CW three-wave mixing in single-mode optical fibers," *J. Appl. Phys.*, Vol. 49, pp. 5098-5106 (1978).
- [9] M. Eiselt, "Limits on WDM Systems Due to Four-Wave Mixing: A Statistical Approach," *J. Lightwave Technol.*, Vol 17, pp. 2261-2267 (1999).
- [10] K. Inoue, K. Nakanishi, K. Oda and H. Toba, "Crosstalk and Power Penalty Due to Fiber Four-Wave Mixing in Multichannel Transmissions," *J. Lightwave Technol.*, Vol. 12, pp. 1423-1439 (1994).
- [11] G. H. Einarsson, *Principles of Lightwave Communications* (John Wiley & Sons, Chichester, 1996).
- [12] P. J. Winzer, M. Pfennigbauer, M. M. Strasser and W. R. Leeb, "Optimum Filter Bandwidths for Optically Pre-amplified NRZ Receivers," *J. Lightwave Technol.*, vol. 19, No. 9, pp. 1263-1273, September 2001.
- [13] B. Xu and M. Brandt-Pearce, "Comparison of FWM- and XPM-Induced Crosstalk Using the Volterra Series Transfer Function Method," *J. Lightwave Technol.*, vol. 21, No. 1, pp. 40-53, January 2003.
- [14] S. Kumar, G. Luther, J. Hurley, "Finite-band noise theory and experiment for four-wave mixing in RZ transmission systems," *OFC*, vol. 3, WW6-1 - WW6-4, 2001
- [15] D. Yevick, "The Accuracy of Multicanonical System Models," *IEEE Photon. Tech. Letters*, 15, 224-226 (2003).
- [16] J. G. Proakis, *Digital Communications* (4<sup>th</sup> ed. McGraw-Hill, New York, 2000).
- [17] K. Inoue, "Phase-mismatching characteristic of four-wave mixing in fiber lines with multistage optical amplifiers," *Optics Letters*, Vol. 17, pp. 801-802 (1992).